Silicon Solar Photovoltaics: Slow Ascent to Exponential Growth

Santosh K. Kurinec

Introduction

Semiconductors such as silicon (Si) and gallium arsenide (GaAs) are materials that generate free carriers and include some organics that generate excitons (which are dissociated to form free carriers) when exposed to photons with energies exceeding their optical bandgaps. The principle of photovoltaics (PV) is that the photogenerated excess carriers get collected by the junction built in electric field and extracted at the contacts, providing useful power output. PV devices and modules made from crystalline silicon currently dominate the market. In a continued quest for lowering their cost, many efforts are being pursued to involve the use of alternative materials and multi-junctions.

The US National Renewable Energy Laboratory (NREL) maintains a plot of compiled values of highest confirmed conversion efficiencies of research cells, from 1976 to the present for a range of photovoltaic technologies [1]. This chart highlights cell efficiency results within different families of semiconductors: (1) multijunction cells, (2) single-junction gallium arsenide cells, (3) crystalline silicon cells, (4) thin film technologies, and (5) emerging photovoltaics. The graph sums up the historic quest of the solar industry to improve the conversion efficiencies in all PV technologies.

The first silicon p–n junction solar cell was fabricated in 1954 at Bell Laboratories [2]. It drew limited attention as it was perceived as a feeble power source. However, the solar cells successfully powered the first Soviet *Sputnik* satellite launched in 1954, triggering the space race. In 1958, the American satellite *Vanguard 1* entered orbit with six silicon solar cells, which generated about 1 watt power in total [3, 4]. In comparison, the power produced by a typical rooftop solar

S. K. Kurinec (✉)
Department of Electrical and Microelectronic Engineering, Rochester Institute of Technology (RIT), Rochester, NY, USA
e-mail: skkemc@rit.edu

M. Bailey, L. Shackelford (eds.), *Women in Mechanical Engineering*, Women in Engineering and Science, https://doi.org/10.1007/978-3-030-91546-9_15

PV system 63 years later is a thousand times greater [5]. Why did it take so long? In contrast, the invention of the first transistor in 1947 took just 11 years to lead to the creation of the first integrated circuit by Texas Instruments, Fairchild, and Intel. The limited momentum of the PV industry was due to the absence of a few dominant players like IBM, Intel, and Motorola, resulting in PV remaining in research laboratories [6]. Most PV interests in the US were for space applications. Growing interest in reevaluating terrestrial applications emerged with the release of small commercial modules by Sharp, Philips, and Solar Power in the early 1970s. The energy crisis and subsequent oil embargoes stimulated the rapid development of PV technology in the mid-1970s, with the first modern modules fabricated in 1976. In 1978, President Carter founded the Solar Energy Research Institute (SERI) in Golden, Colorado, and later in 1991, President George H. W. Bush elevated SERI to a national member of the Department of Energy (DOE)—National Renewable Energy Laboratory (NREL).

After dramatic achievements in module designs supported by the US Government programs, declining funding and interests shifted the key research and development to other countries in Europe, Japan, and Australia. Martin Green, PV pioneer and world-leading specialist in crystalline silicon solar cells, founded in University of New South Wales, the largest and best-known university-based photovoltaic research group in the world in 2003 [5, 7]. Remarkable progress was made with cells on high-quality monocrystalline, multicrystalline (Generation I), and thin film amorphous silicon, while III–V GaAs-based single junction and multi-junction solar cells were investigated for space-based applications. Generation II, III, and IV photovoltaics include thin film, multi-junction, multiband, hot carrier, and perovskite-based solar cells and all these technologies are promising, showing record efficiencies. For terrestrial applications, cost, environmental stability, and long lifetime with minimum degradation (>25 years) are the key factors. The US DOE SunShot initiative was launched in 2011 with a goal of cost reduction of utility-scale solar to approximately $1 per watt or $0.06 per kilowatt-hour. The program is now at 90% of its goal and recently expanded its target to $0.03 per kilowatt-hour by 2030 [8]. This chapter provides a comprehensive overview of silicon photovoltaics and my experiential journey encountering its reluctant ascent to a dominating technology.

Brief Historical Lookback

My interest in Physics sparked when my science teacher in high school tenth grade taught about the peaceful use of nuclear energy using controlled nuclear fission for power generation. I decided to pursue a BS and MS in Physics at the University of Delhi. I interned at the nuclear research reactor of Bhabha Atomic Research Center, India, during a summer of my Master's program. After graduating, I joined the National Physical Laboratory (NPL), New Delhi, India, for my PhD research. India was exploring the development of magnetic materials for booming electrical, electronics, and automotive industries, using indigenous raw materials.

Dust in Rust

Iron oxide is the main raw material used in magnetic ceramics like ferrites. Silicon dioxide is a common impurity in indigenous iron oxide. My PhD research was focused on understanding the effect of silicon impurity on the magnetic properties of Mn–Zn ferrites. The Indian Institute of Technology in Delhi had acquired its first scanning electron microscope (SEM) from Cambridge Instruments (Cambridge Stereoscan S4–10 SEM). I employed it to examine microstructures by imaging secondary electrons, electron dispersive diffraction (EDX), and electron beam induced current (EBIC) modes. It was found through detailed microstructural examinations that a certain level of silicon is soluble in the ferrite and, in fact, improved the magnetic properties. When it exceeds solid solubility, it segregates at grain boundaries, degrading the magnetic properties such as permeability and loss factor. Figure 1 shows SEM and EDX image of a Mn–Zn ferrite sample showing Si segregation at the grain boundaries [9]. At the time I finished my PhD, the energy crisis was being felt worldwide, directing a focus on renewables. Major research institutions drew attention to photovoltaics.

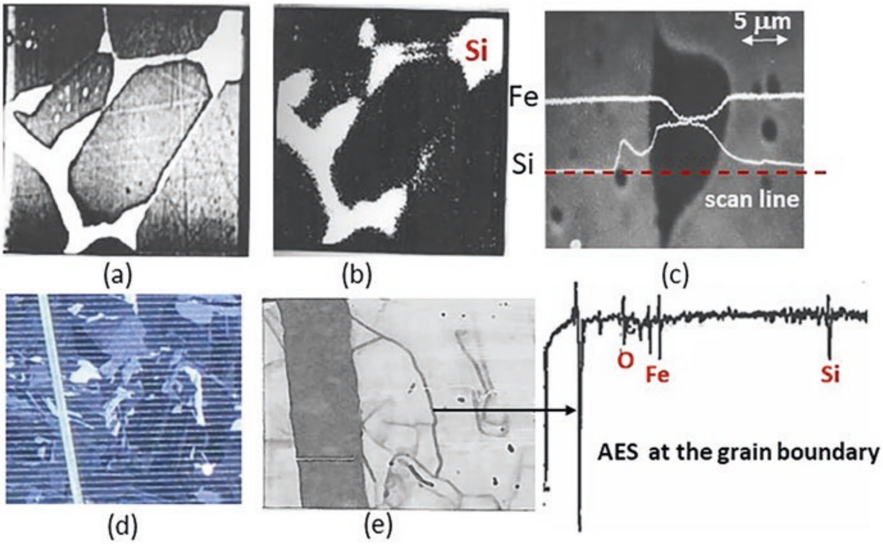

Fig. 1 SEM (**a**) and EDX map and line scans (**b**, **c**) of Mn–Zn ferrite grain showing Si segregation at the grain boundaries; (**d**) mc-Si solar cell examined at a grain boundary using Auger Electron Spectroscopy (AES) showing Fe segregation at the Si grain boundary

Rust in Dust

The Department of Materials at NPL set up a complete process for purification of metallurgical grade silicon obtained from a regional steel plant. It consisted of reacting silicon with HCl to get liquid trichlorosilane (TCS), which was fractionally distilled to purify to solar grade level. After purification, TCS was cracked in a reactor to get polycrystalline silicon (polysilicon) rods. On the industrial scale, it is known as the Siemen's process and is the flagship process for silicon purification developed in the early 1980s. The polysilicon rods were zone-refined for compaction and we obtained large grain polysilicon rods (Fig. 2). Then, wafers were cut, lapped, and polished. The wafers were *n*-type as the silicon obtained was rich in phosphorus. We had in-house doping techniques using solid paper and liquid spin-on dopant sources. Solar cells were fabricated with Al/Ag and Ti/Al/Ag metallization yielding 10% efficiency [10]. Detailed analyses revealed significant iron impurity in silicon that affects the PV quality of the material. My research in PV began with investigating the effect of iron impurity in multi-crystalline silicon solar cells.

TAET Program

The University of Florida and the US Agency for International Development established a training program in Alternative Energy Technologies (TAET) in the 1980s. The TAET program provided training in both the technical principles and socioeconomic aspects of the selection and implementation of renewables. In 1982, I was selected as a participant from India among 35 participants from around the world. I carried out a project on investigating the nature of grain boundaries and their influence on the photovoltaic properties of polysilicon. This work attracted me to join the University of Florida as a Postdoctoral Research Associate to further my PV research.

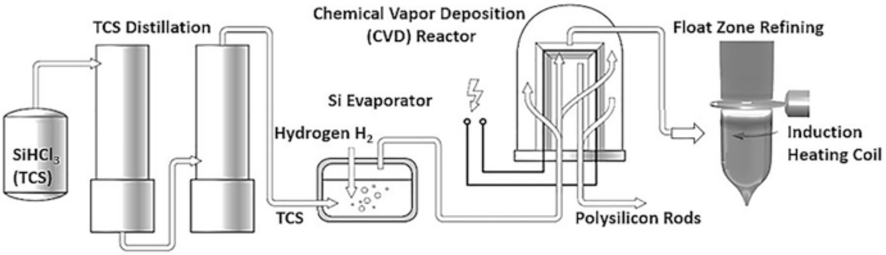

Fig. 2 In-house developed silicon purification process followed by float zone refining, used at NPL to fabricate mc-Si solar cells of 10% efficiency

Photovoltaics

The solar spectrum is modeled as a black body radiation emitted by the Sun at its surface temperature of 5800 K according to Planck's law. The reference Air Mass 1.5 (AM1.5) spectrum describes solar insolation on a terrestrial horizontal surface at a solar zenith angle of 48.19° and it is specified as 1 kW/m^2. In a single junction diode solar cell, incident photons with energy equal or higher than the bandgap of the semiconductor create electron hole pairs, which are collected by the junction electric field. This gives rise to radiation-generated current, shifting the diode current–voltage curve to power generation mode. Figure 3 shows a baseline cell fabrication process, electrical equivalent circuit, and current–voltage characteristics of a solar cell. The power conversion efficiency is defined as the ratio of the maximum power generated to the incoming incident power.

Shockley and Queisser obtained the theoretical limit to the conversion efficiency through detailed balance limit of p–n junction solar cells on the basis of absorption and reemission processes [11]. AM1.5 solar spectrum with distinct dips due to molecular absorption in Earth's atmosphere is shown in Fig. 4a. Photons with energies below the band gap (E_g) are not absorbed, whereas the energy of photons with energy higher than the band gap is not fully converted to electrical energy and is dissipated as the thermalization loss. The inset in Fig. 4a depicts the electronic band structure with the separation of the quasi-Fermi levels determining the open-circuit voltage V_{oc}. Theoretical Shockley–Queisser detailed-balance efficiency limit as a function of band gap (black line) is shown in Fig. 4b. The record efficiencies for different materials are plotted for the corresponding band gaps. An optimum bandgap (~1.4 eV) gives the highest theoretical limit of the efficiency as 33%. NWO-I Institute for Atomic and Molecular Physics, Netherlands, constantly updates this efficiency chart [12].

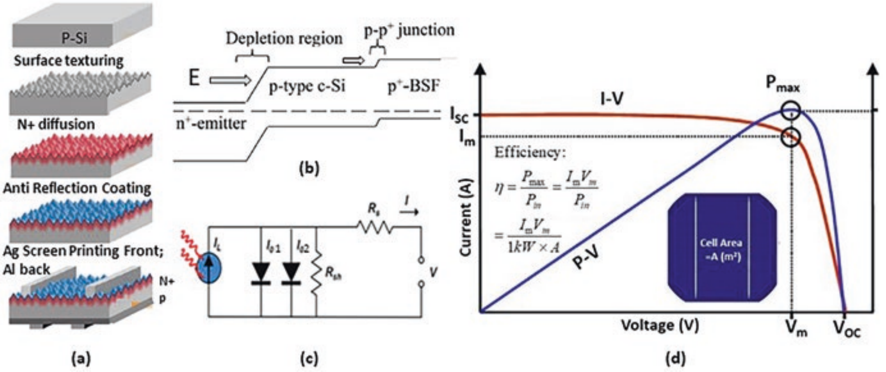

Fig. 3 (**a**) Process flow for a basic n + p solar cell; (**b**) equilibrium band diagram of n+pp.+; (**c**) a two diode equivalent circuit of a solar cell; (**d**) typical current–voltage characteristics of a solar cell defining the key parameters: open circuit voltage (V_{oc}), short circuit current (I_{sc}), maximum power (P_{max}), and power conversion efficiency

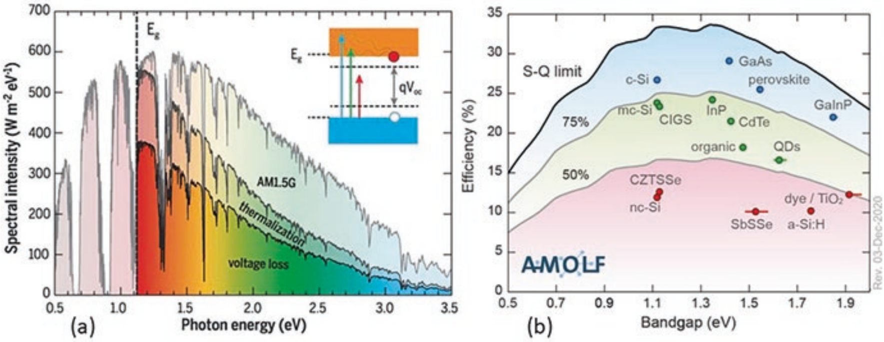

Fig. 4 (**a**) AM1.5 solar spectrum and (**b**) fundamentals solar cell efficiency limits [12]. (Reprinted with permission)

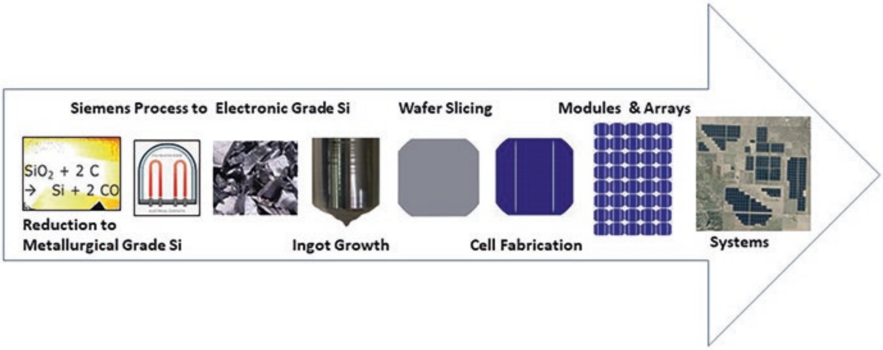

Fig. 5 Process flow chart for fabricating monocrystalline silicon solar PV systems

Crystalline silicon with the bandgap of 1.12 eV has this limit of ~30%. Silicon is the second most abundant element on the Earth, and mostly exists as oxide (SiO_2, or silica). Silicon has the diamond crystal structure and is chemically stable, nontoxic, and very well understood as the base semiconductor for microelectronics. It forms a very high-quality oxide, which is used as passivation and dielectric component and masking layer for patterning diffusion of dopants.

Figure 5 shows a flowchart of manufacturing silicon photovoltaics starting from sand. It begins with a highly energy-consuming process of carbon arc reduction of SiO_2 to metallurgical-grade Si (~98% pure). It is then purified, grown with crystalline structure, followed by wafering, cell and module fabrication. Each step requires process optimizations for efficiency improvements and cost reductions.

Innovations in Si PV

Over the last several decades, academics, scientific laboratories, and niche industries worldwide have remained diligently committed in achieving higher efficiencies across cell, module, and system level. These accomplishments are summarized in the following subsections.

Cell Level

The simplest form of a solar cell is a p–n junction connected with grid top metal and blanket back metal contacts as shown in Fig. 4a. In order to improve the efficiency, approaches to reduce reflection losses, optimization of diffusion, improved minority carrier lifetimes, and reduction of parasitic resistances were necessary. These improvements required novel cell structures. A series of high-efficiency crystalline silicon solar cell structures have emerged, which include passivated emitter rear cell (PERC), passivated emitter, rear locally diffused cell (PERL), interdigitated back contact cell (IBC), heterojunction with intrinsic thin-layer cell (HIT), heterojunction solar cells with interdigitated back contacts (HBC), bifacial cells, and TOPCon solar cells [13, 14]. When deployed on a conventional solar farm, bifacial cells absorb direct incoming light, while also taking advantage of ground reflection, which can contribute up to additional 30% power generation [15]. PERC cells with another addition of a special nano-coating layer, known as Q cells, can capture previously unused sunlight back into the cell where it can be converted into solar electricity [16]. It enhances cell efficiency further. Table 1 gives the schematics of these structures and their best known efficiencies to date.

The first efficient silicon solar cell was made on a n-type substrate. The selection of p-type as the substrate was primarily due to the development of Al-BSF process that creates back surface field (BSF) to mitigate minority carrier recombinations at the back contact. On a per-watt basis, passivated emitter and rear totally diffused, silicon heterojunction (SHJ or HIT), and interdigitated back contact cells currently cost more than standard aluminum back surface field (Al-BSF) and PERC cells owing to smaller production scales and use of n-type wafers [14]. However, if demand for high-efficiency cell architectures grows, these advanced cell technologies may gain market share and their cost may decline due to benefits from economies of scale. Cells with higher efficiencies could reduce per-watt balance-of-module and balance-of-system costs [17].

Table 1 Record reported efficiencies in single junction silicon solar cells (as of 2020)

Solar Cell Type	Cross-section Schematic	η	Solar Cell Type	Cross-section Schematic	η
I. Passivated emitter rear cell (PERC)- Mono • 'Workhorse' of the PV industry today **PERC- Multi**	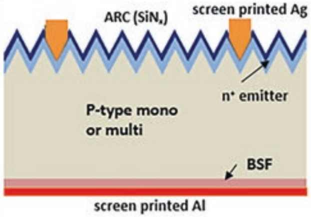	24 22	**IV. Interdigitated back contact cell (IBC)** • Both electrodes at rear side, no shading • High demands on material quality. Carriers must travel through complete wafer. Excellent passivation required: low front surface recombination velocity • Challenges:defining and separating both polarities on same side	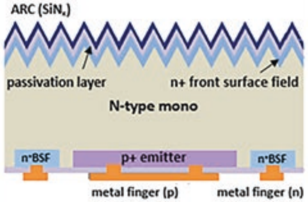	22.5
II. Bifacial PERL • Increased power generation due to additional rear side illumination. • Can be made PERC as well	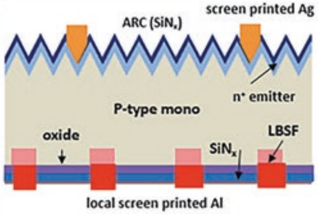	22	**V. Heterojunction solar cells with interdigitated back contacts (HBC)**	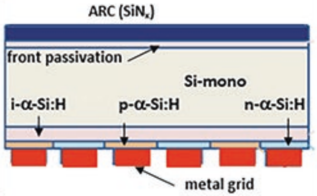	26.7
III. Heterojunction with intrinsic thin-layer cell (HIT) • Cells make use of passivating contacts based on a layer stack of intrinsic and doped amorphous silicon	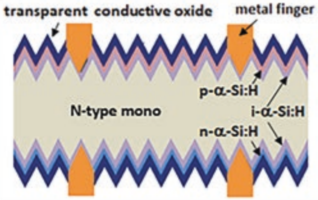	25.1	**VI. TOPCon solar cells** • Carrier selective, thin SiOx tunnel oxide to passivate rear contact • Heavily doped pseudo-crystalline Si transport layer • No rear side patterning required • Low contact resistance, high FF • One-dimensional flow of charge carriers	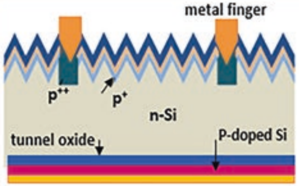	25.7

Substrate Level

Solar-grade polysilicon typically has purity levels of 6N (99.9999% pure) to 8N (99.999999%) and it is used to make solar cells; 9N polysilicon may also be used in some premium solar cells. Electronic-grade polysilicon has higher purity levels of 9N to 11 N for producing silicon wafers for integrated circuits. The Siemens process, mentioned above, is the most widely used method for polysilicon production. Polysilicon sits on top of the photovoltaic supply chain. One megawatt (MW) of photovoltaic power requires 7 tons, or 7000 kg, of polysilicon material [18].

Polysilicon is cast into monocrystalline (mono-Si) or multicrystalline (mc-Si) silicon. Mono-Si is grown using the Czochralski (CZ) crystal growth process. At the beginning of the CZ process, the polysilicon is melted in a cylindrically shaped crucible. After the feed material is completely molten, a seed crystal with a diameter of typically a few millimeters is dipped from top into the free melt surface forming a melt meniscus at the contact interface between seed and melt. Then, the seed is slowly withdrawn from the melt (often under rotation) and the melt crystallizes at the interface by forming a new crystal portion. During the further growth process, the shape of the crystal, especially the diameter, is controlled by carefully adjusting the heating power, the pulling rate, and the rotation rate of the crystal [19]. Silicon ingots are cylindrical giving circular wafers, which require a larger surface area of a solar panel compared to square-shaped. Multicrystalline silicon (mc-Si) is produced by melting Si and directionally solidifying into bricks. The mc-Si process yields rectangular wafers, which can be packed densely on a panel. The production of mc-Si is cost efficient compared to the mono-Si CZ process and therefore has prevailed as a major technology for the solar panels. However, the defects present in the mc-Si because of the production process lead to less-efficient solar cells.

Thinner wafers are preferred to lower the cost and the weight of the panels. While the technical limit of slurry-based wire saws lies at a wire thickness of 100 µm, diamond wire can be as thin as 60 µm and thus reduce the kerf loss significantly [20]. The cylindrical ingot is first cut along its length on four sides to make its shape closer to a square in cross section, known as the pseudo squares. Pseudo square diameter is the diameter of a square within a circle. Wafer sizes have increased over the last 7 years from M0 (156/205 mm, flat length/diagonal length) to M2 (156.75/210 mm), and to M6 (166/223 mm). Larger wafer size offers balance of systems cost reductions. For installation, a 72-M6-cell module weighs around 30 kg, which is near the limits of manual installation. Considering the increased power output, including potential bifacial gains, the M6 wafer will increase the operational current to around 13 amps, which is the limitation of current string inverters. Modules using M6 wafers are also compatible with centralized inverters [21].

In August 2019, Zhonghuan Semiconductor unveiled its latest wafer product—the new M12 size—featuring a much bigger size of 210 mm in length and 295 mm on the diagonal [22]. A 60-cell PV module with this enlarged wafer would easily boost module power output above 600 W. M12 is targeting next-generation PV cell technologies such as interdigitated back contact technology. Figure 6 shows a picture of a wafer puller capable of pulling M10–M12 ingots developed by Linton Crystal Technologies [23], a Rochester, New York–based company. This puller employs the Magnetic Confined Czochralski method that lowers oxygen contamination in the crystal.

Most PV modules are fabricated using p-type silicon substrate, which is highly susceptible to light-induced degradation (LID) when exposed to sunlight. Boron-doped p-type silicon thus requires additional processing steps to mitigate this degradation [24]. An alternative method for the production of stable lifetime material is to dope silicon with a different Group III element, such as aluminum, gallium, or indium. Gallium is being explored as the dominant dopant for p-type silicon solar cells [25]. However, it has much lower segregation coefficient ($k = 0.008$), which means that gallium has a much stronger thermodynamic tendency to stay in the melt rather than be incorporated into the solid silicon crystal. One way to overcome this is to constantly replenish the melt with gallium during the crystal growth to achieve uniform resistivity (1–2 Ohm.cm) along the crystal. Another method being considered is the Continuous Czochralski method, which does not require a large crucible as Si is fed while the ingot grows [26].

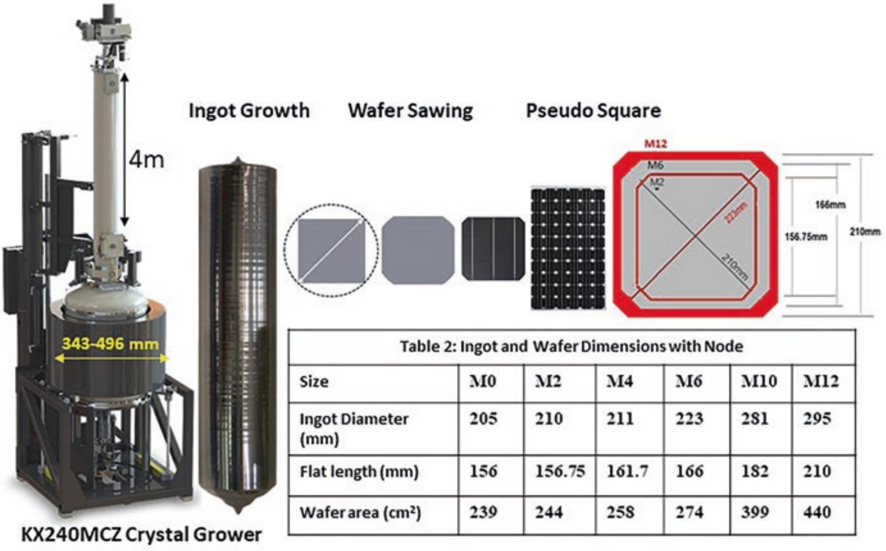

Table 2: Ingot and Wafer Dimensions with Node

Size	M0	M2	M4	M6	M10	M12
Ingot Diameter (mm)	205	210	211	223	281	295
Flat length (mm)	156	156.75	161.7	166	182	210
Wafer area (cm²)	239	244	258	274	399	440

Fig. 6 Czochralski (CZ) crystal puller (Courtesy: Linton Crystal Technologies) designed to grow M10–M12 ingots. Circular wafers are shaped into pseudo squares with dimensions shown in Table II for each generation

Modules

Solar cells are connected in series and parallel to construct modules for required voltage, current, and power output. Series connection adds voltages and parallel connections add currents of individual identical cells. Typically, PV modules are fabricated by electrically connecting 36 to 72 solar cells together in a sealed, weather-proof packaging and are the fundamental building block of a PV system [27].

Mismatch occurs when some cells degrade in their performance due to shading effects or other degradation causes. Series strings are more prone to shading effects and therefore bypass diodes are used to allow bypassing current through the damaged cell. Solar cells transport current using the thin metal ribbons that connect them to neighboring wires and cells, which leads to some energy lost. By cutting solar cells in half, the current generated from each cell is halved resulting in lower interconnect resistive losses. Two parallel half-cut cell strings replace one full cell series string. Half-cut cell modules increase module power by ~1.5% due to reduced electrical losses in cell connectors. Parallel substrings allow the module to save up to 50% of the string's power under partial shading conditions [28].

Another simple and accessible way to reduce resistance losses in solar cells is to add more busbars. Adding more busbars reduces the gap between them, which shortens the finger length. The forthcoming trends are—increasing the number of busbars, while maintaining the same shading factor, and switching to multi-busbars using round wires (9–15 wires) instead of flat ribbons as interconnections [29]. The round-shaped busbar, a wire indeed, increases the light scattering effect towards the cell surface for higher cell absorption, resulting in increased power generation.

Most bulk silicon PV modules consist of a transparent top surface, an encapsulant, a rear layer, and a frame around the outer edge [27]. The main attributes of glass used are transmission, mechanical strength, and specific weight. The front surface of a Si PV module must have a high transmission in the wavelength range of 350–1200 nm. In addition, the reflection from the front surface should be low. Currently, 3 mm–thick glass is the predominant cover material for PV modules accounting for 10–25% of the total cost. The cover glasses can also provide enhanced ultraviolet protection of polymeric PV module components, potentially increasing module service lifetimes [30]. The properties of PV module materials are of great importance to ensure optimal light capture and module lifetime as well as ultimately reducing the cost. Traditional opaque-backsheeted panels are monofacial. Bifacial modules expose both the front and backside of the solar cells. When bifacial modules are installed on a highly reflective surface (like a white thermoplastic polyolefin roof or on the ground with light-colored stones), gains can be up to a 30% increase in power production just from the extra power generated from the rear [31]. Fig. 7 shows a PV system under installation at City Center Bishop Ranch, California, that I recently visited to learn the installation processes.

Fig. 7 Bifacial horizontal roof top solar arrays using 12 multi-busbar mono-Si modules (left); inclined half-cut 6 busbar Q-cells panels (right) under installation at Bishop Ranch, California. Single panel and cell schematics are shown. (Photo courtesy Distributed Solar Development)

PV Systems

A stand-alone PV system is made up of a number of individual PV modules (or panels) usually of 12 V with power outputs of between 50 and 300+ W each. These PV modules are then combined into a single array to give the desired power output. A small-scale PV system employs rechargeable batteries to store the electrical energy supplied by the PV array. Stand-alone PV systems are ideal for remote rural areas and applications where other power sources are either impractical or are unavailable to provide power for lighting, appliances, and other uses. In these cases, it is more cost-effective to install a single stand-alone PV system than pay for the costs of extending power lines and cables. Residential PV systems (4–10 kW) are grid connected and some may have additional battery storage (Fig. 8). Production and consumption is metered using net metering systems. Utility-scale PV systems are community shared via the grid. For hundreds of megawatt-scale solar farms, how will electricity get from large solar farms to cities? At present, the majority of high-voltage transmission lines are alternating current, but recent innovations suggest they are increasingly likely to be high-voltage direct current (HVDC) lines. HVDC are cheaper at longer distances over land and at very short distances underwater and underground [32]. This means that HVDC will enable electricity to travel long distances from renewable locations, connecting islands to the mainland and even continents to one another potentially.

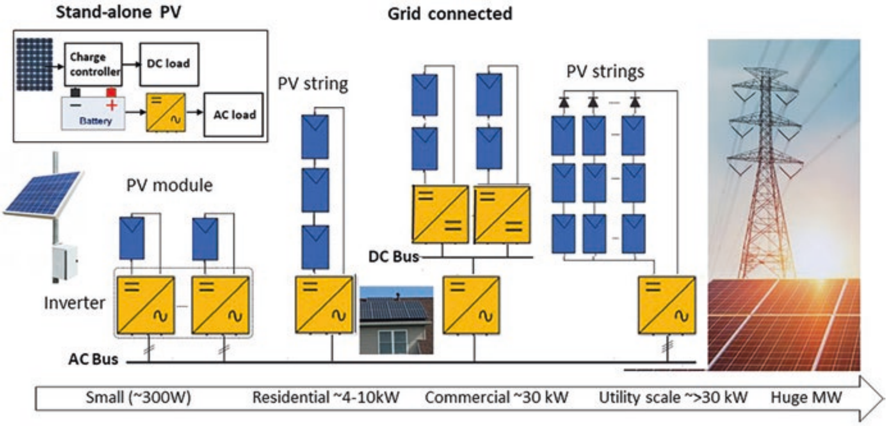

Fig. 8 PV systems ranging from stand-alone to grid connected residential, commercial, and utility scale systems

My Research at the Photovoltaics Microelectronics Intersection

While I was working on polysilicon for PV, the semiconductor chip industry was looking to use polysilicon as the gate material in complementary metal oxide semiconductor (CMOS) field-effect transistors for integrated circuits. In addition, interests in photodetectors and light-emitting diodes emerged for optical interconnects when the Strategic Defense Initiative "Star Wars" was announced (1983) [33]. Many PV researchers moved to these fields, including myself. Since then, my research and teaching has been in both semiconductor devices and photovoltaics.

The growth of innovative techniques that enabled the integrated circuit technology to become efficient in the high volume manufacturing of extremely small and complex systems (with nanometer-scaled billions of stacked devices) on large substrate, set up a sound base for the PV industry. Between the two, they share a common substrate—silicon and common thin film deposition techniques. PV contrasts itself from CMOS in being relatively simpler in device structure (essentially one large area ~ 250 cm^2 diode), relaxed in lithography and particle contamination controls. However, it differentiates in applications that require large area end-products, much larger than the flat panel displays, and is available at lower costs. Even though the PV industry inherits an experienced workforce trained in defining and following the roadmap driven by the Moore's law, engineering education needs to address developing the next generation of PV engineers.

I developed a cross-disciplinary course—"Photovoltaics Science and Engineering" at the graduate/senior undergraduate level in the college of engineering at Rochester Institute of Technology (RIT) in 2007. Students from various programs—electrical, microelectronic, chemical, materials science, industrial engineering, and physics—have enrolled in this course and many students have moved on to the PV industry, PhD in PV-related areas, and published papers and chapters in these areas [26, 34]. The following subsections ("Cell Level", "System Level" and "Spectrum Conversion") summarize my PV-related research.

Cell Level

At RIT, we developed a turnkey process for fabricating solar cells—a platform that was intended to investigate different approaches in diffusion, metallization, and top-surface reflectance [35]. During my sabbatical at IBM Watson Research Center in 2009, I investigated upgraded metallurgical-grade silicon for solar cells using this turnkey process.

The University of North Carolina and Georgia Tech founded the Silicon Solar Consortium, an Industry–University Cooperative Research Center in 2007. My group joined this consortium and worked on developing copper metallization to replace silver in silicon solar cells. Silver represents >48% of the metallization cost of a solar cell, or about 11% of the total raw material cost of a solar module. Copper presents a viable alternative to silver with the potential to reduce metallization costs by approximately 50% while maintaining device performance in solar cells. The primary concern with copper is its rapid diffusion in silicon, lowering the minority carrier lifetime, and therefore greatly diminishing the efficiency of the device.

IBM rocked the microelectronic industry by implementing copper as the interconnect metal in integrated circuits in 1997, as copper was undesirable due to its fast diffusion in silicon and difficulties in etch patterning. Special liners, diffusion barriers, electroplating, and patterning by chemical mechanical planarization processes were developed. Copper interconnects have since become the industry standard, enabling future generations of smaller and faster microprocessors.

Some metal silicides ($TiSi_2$, $CoSi_2$, NiSi) exhibit low resistivity and higher temperature process capability compared to aluminum which was used as the gate electrode in early days in integrated circuits. Self-aligned silicide process was developed in the mid-1980s that reduced gate and contact resistance by using metal silicides. Silicides are formed by metal deposition on silicon followed by annealing to form the desired low resistivity phase. Nickel monosilicide (NiSi) with a resistivity of 10–18 μΩ.cm consumes less silicon during its formation, and is widely used in ICs.

NiSi is a strong contender as a contact, as it shows promise as a copper diffusion barrier. My group studied the NiSi/Cu contacts for front metallization of silicon solar cells [36]. NiSi/Cu/TiN contacts with contact resistivities as low as 4×10^{-5} Ω-cm^2 were formed to the emitter of solar cells fabricated at RIT and 2×10^{-3} Ω-cm^2 on NREL fabricated tunneling contacts [37]. Contact resistance is related to the metal semiconductor specific contact resistivity, which is the fundamental property of a metal–semiconductor junction. We investigated the effects of transmission line measurements (TLM) geometries on the extracted value of specific contact resistivity [38]. This work, in collaboration with Professor Zhang, Michigan State University, and Professor Kris Davis, University of Central Florida, led to the development of standardized TLM structures for specific contact resistivity measurements.

System Level

System Monitoring

The Golisano Institute for Sustainability (GIS) building at RIT is equipped with mc-Si PV modules with an annual capacity of 45,241 kW-h. In our study (with my graduate student Felipe Freire), yearly power output of the GIS PV system was investigated using a mathematical model developed and comparing with real data collected from the monitoring system. The objective was to predict PV modules' performance with respect to changes in environmental parameters such as temperature, irradiance, and cloud coverage. The results were compared with the actual PV output data for the year 2014 and showed a very good correlation [39]. This mathematical model has been applied to several PV systems with known parameters—location, time of the day, panel orientation, and weather conditions.

Interestingly, it was used to explain the power dip in a residential PV system during the partial solar eclipse of August 21, 2017 [40]. The solar coverage was calculated using astro-imaging the Sun during the eclipse and calculating insolation over the eclipse time (Fig. 9). Strange coincidence, during the February 16, 1980, eclipse in India, as a student, I monitored a solar cell short-circuit current to provide insolation data to researchers investigating cosmic flux of gamma rays during the eclipse.

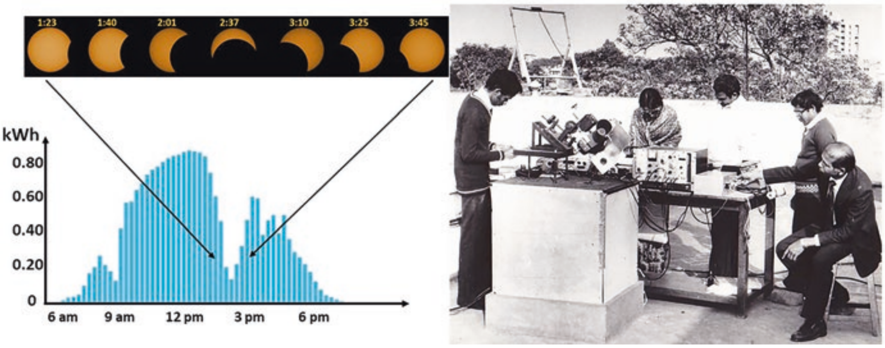

Fig. 9 Power output of a residential PV system during the partial eclipse of August 21, 2017 (left); monitoring solar insolation using a solar cell to calibrate cosmic gamma ray flux during the eclipse of February 16, 1980

PV Degradation

PV modules are considered the most reliable component of a photovoltaic system, and according to the manufacturers, have a lifetime from 25 to 30 years. However, some modules degrade or fail along their service time under outdoor exposure. To further understand the mechanisms behind the degradation and failure of PV modules, our study reviewed the governing degradation modes and investigated a 10-year-old operating crystalline silicon PV module installed at an active farm and animal sanctuary [41]. Field current–voltage testing and infrared imaging for hotspot detection were employed in examining this PV module showing localized damaged regions.

Spectrum Conversion

Currently, I am working on photon management techniques to enhance power conversion efficiencies. Development of special coatings that can shift the spectrum toward the favorable wavelengths would result in enhanced power output. For Si PV, down conversion of shorter wavelengths to longer wavelengths, which give higher quantum efficiency, is desirable. This is fostering innovations in photonic coatings. In collaboration with a startup company—SunDensity [42]—we have demonstrated increase in power output of a high efficiency PERC Si solar cell (Fig. 10) using a designed special coating.

Silicon Photovoltaics from Present to Future

The primary ambition of PV is to offer a cheaper, reliable, and resilient renewable energy alternative. The motivation and willpower for large-scale implementation of PV has been steering the innovations in materials, devices, and systems. Following the unprecedented growth and success of the semiconductor industry, the PV industry has its own “Moore’s law.” Figure 11 shows the advances in wafer sizes and cells in module architectures.

Table 2 lists and defines some key figures of merits (FOM) indicators and their current estimated values. The key economic FOMs are the payback time (PBT), the energy payback time (EPBT), and carbon payback time (CPBT). Depending on the technology and location of the PV system, the EPBT today ranges from 0.4 to 1.5 years [43]. Energy return on investment (EROI) is defined as the lifetime energy output to the energy invested. In general, on the average solar panels are estimated to generate ten times more energy than used to make them [44]. A typical solar panel saves over 900 kg of CO_2 per year resulting in a carbon payback period of ~1.6 years [45].

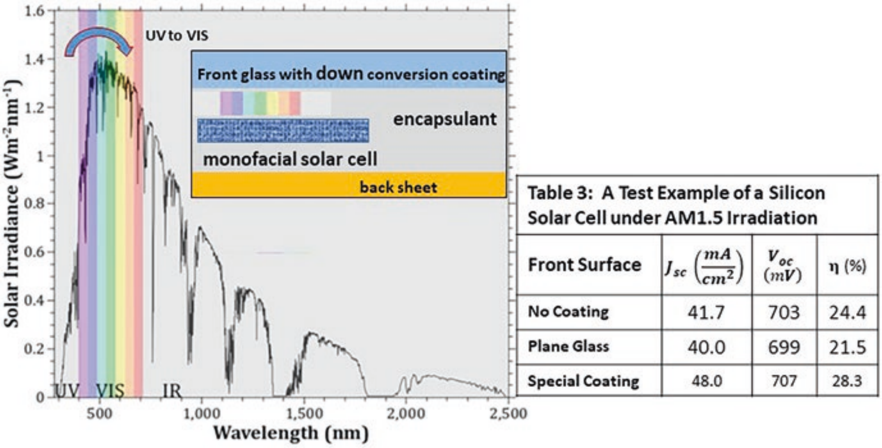

Table 3: A Test Example of a Silicon Solar Cell under AM1.5 Irradiation

Front Surface	$J_{sc}\left(\frac{mA}{cm^2}\right)$	V_{oc} (mV)	η (%)
No Coating	41.7	703	24.4
Plane Glass	40.0	699	21.5
Special Coating	48.0	707	28.3

Fig. 10 Spectrum down conversion using a special coating (developed by SunDensity) tested for a high efficiency Si solar cell

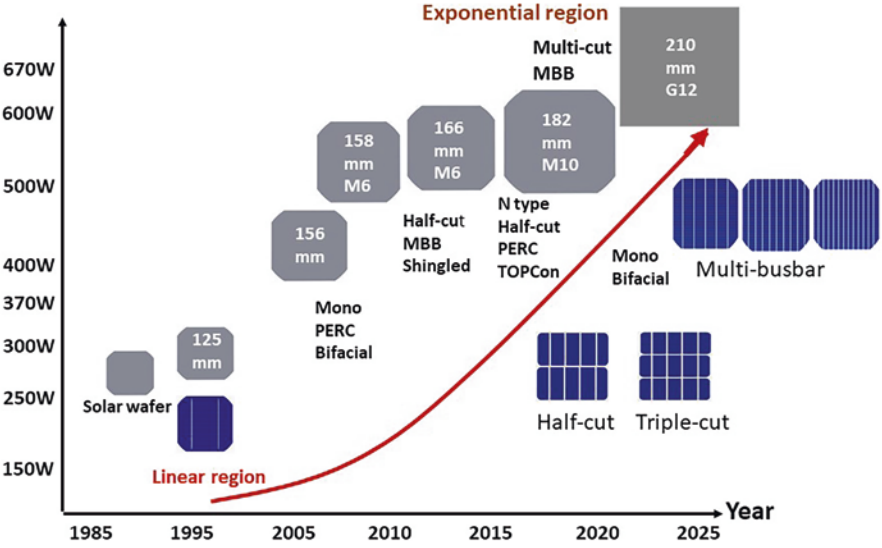

Fig. 11 Trends in silicon PV wafer sizes, emerging cell architectures toward bifacial, multi-busbar, and multi-cut modules

The cumulative PV installations from 2010 to 2020 are reaching 800 gigawatt-peak (GWp) (Fig. 12) [46]. A 2019 review in *Science* led by researchers from NREL describes an ambitious plan, in which 30–70 terawatt (TW) of PV capacity making it a central contributor to all segments of the global energy system by 2050 [47].

Most energy forecasters suggest that the installed cost of a complete PV system, including modules and balance of system (BOS) components will need to fall below

Table 2 Economic/environmental performance indicators for Si PV

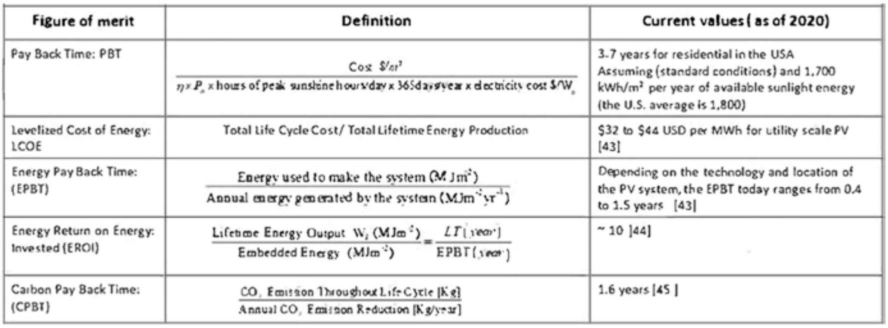

Figure of merit	Definition	Current values (as of 2020)
Pay Back Time: PBT	$\frac{\text{Cost } \$/m^2}{\eta \times P_a \times \text{hours of peak sunshine hours/day} \times 365\text{days/year} \times \text{electricity cost } \$/W_p}$	3-7 years for residential in the USA Assuming (standard conditions) and 1,700 kWh/m² per year of available sunlight energy (the U.S. average is 1,800)
Levelized Cost of Energy: LCOE	Total Life Cycle Cost/ Total Lifetime Energy Production	\$32 to \$44 USD per MWh for utility scale PV [43]
Energy Pay Back Time: (EPBT)	$\frac{\text{Energy used to make the system } (MJm^{2})}{\text{Annual energy generated by the system } (MJm^{-2}yr^{-1})}$	Depending on the technology and location of the PV system, the EPBT today ranges from 0.4 to 1.5 years [43]
Energy Return on Energy: Invested (EROI)	$\frac{\text{Lifetime Energy Output } W_l\ (MJm^{-2})}{\text{Embedded Energy } (MJm^{-2})} = \frac{LT\,(year)}{EPBT\,(year)}$	~ 10 [44]
Carbon Pay Back Time: (CPBT)	$\frac{CO_2 \text{ Emission Throughout Life Cycle [Kg]}}{\text{Annual } CO_2 \text{ Emission Reduction [Kg/year]}}$	1.6 years [45]

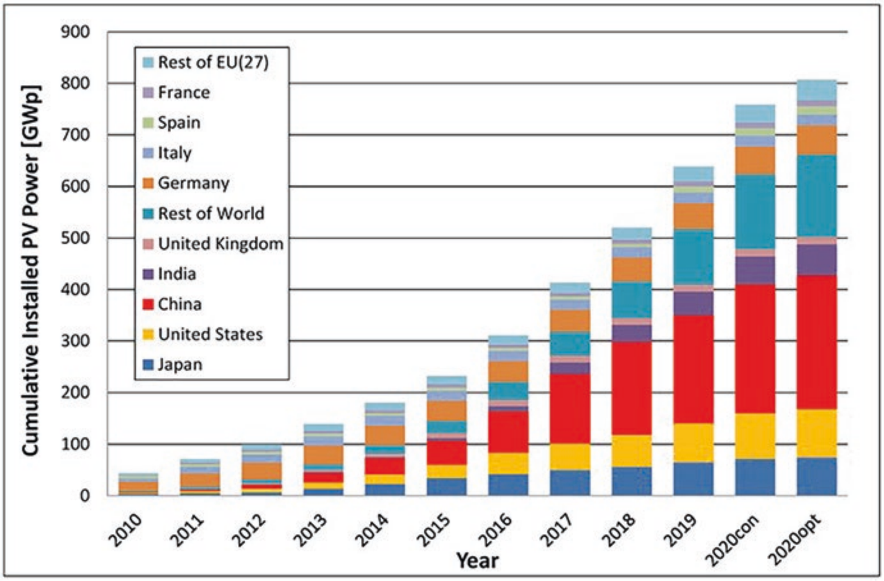

Fig. 12 Cumulative photovoltaic installations from 2010 to 2020 [46]

\$0.25 per watt for this goal. NREL's 2019 roadmap for continued innovations anticipates that the cost of crystalline silicon modules will decline to 0.24 per watt by 2030.

The International Energy Agency (IEA) Renewable 2020 reports that power generation from solar PV is estimated to have increased by 22% in 2019 to 720 TWh. Solar PV is well on track to reach the Sustainable Development Scenario level by 2030, which will require electricity generation from solar PV to increase 15% annually, from 720 TWh in 2019 to almost 3300 TWh in 2030 [48]. In 2019, PV generation overtook bioenergy and is now the third-largest renewable electricity technology after hydropower and onshore wind.

A major renewable energy project in Australia billed as the world's largest solar farm is in development. The farm will have a peak capacity of around 10-GW and will spread across an area of roughly 20,000 football fields! That is so large that it should be visible from space, once built. The project aims to transport its solar energy to Singapore using a 4500 km high-voltage direct current network, 3700 km of which will be undersea. It is projected that the project will be able to provide up to 20% of Singapore's power needs. Construction is expected to commence in 2023, with the farm expecting to begin exporting energy by 2027.

The intermittency of solar PV requires smart energy storage and dynamic power distribution systems. Hardware and software innovations will play a key role in managing storage resources, shifting capacity during peak periods, providing secondary services in the off-peak hours and standby power for emergencies.

Conclusions

Growing up during the Cold War, my interest in energy began with learning how nuclear reaction can be used for energy production. Nuclear energy technology with its high capacity factor and zero carbon emission, however, has the perception of safety risks. As we moved to the energy crisis era of the 1970s, interest in PV emerged. Subsequently, the growth of semiconductor technology dominated, leading to the Internet revolution. At present, energy consumption in computing is increasing super exponentially. My current work on semiconductors is also dedicated to energy-efficient computing devices. I foresee a future—using nuclear power plants for silicon production and solar cell manufacturing, and solar PV farms powering the energy-hungry data centers.

I have experienced the Si PV journey over the last four decades. Attention on Si PV got accelerated, slowed down, and recovered primarily due to economic circumstances. While major research innovations were achieved in the US, Europe, Japan, and Australia, China took the lead in manufacturing and currently shares 95% of the market share.

Today, Si-based solar PV cells are becoming more affordable and are being installed in large numbers with gigawatt (GW)-scale solar farms. Larger area mono-Si cells with advanced cell designs, multi-busbars, are being incorporated on multi-cut modules. Trends toward heterojunction with intrinsic thin layer (HIT), bifacial, and interdigitated back contact cells are promising. Just recently, scientists at The Australian National University (ANU) have produced a type of bifacial Si solar cell, using laser processing, setting a new world record effective power output of approximately 29%, well exceeding the performance of the best single-sided silicon solar cell [49]. On the other hand, major market players are likely to invest more in research and development to increase the efficiency of photovoltaic cells and find more effective material than silicon to build solar cells. However, these improvements will take time and are possible only if solar cells undergo bulk manufacturing and installations. In addition, although c-Si remains the dominant PV technology, it would need to continue to compete against evolving alternative PV technologies such as cadmium telluride (CdTe), copper indium gallium diselenide (CIGS), and perovskite modules. This competition will likely drive innovations for cost reductions across all technologies while presenting additional opportunities for system optimizations. Si PV may be augmented with multi-junction approaches with other semiconductors if the processes can be large-area centric and environmentally stable over the lifetime. Moving forward, new chemical approaches may be needed to make sand-to-Si reduction process more energy efficient [50]. Silicon is resilient. A 42 year-old, 42 W, 3.5 A, 12 V Kyocera solar panel exposed to environment is still reported to be working in Concord, NH [51]. *Silicon PV has become "too big to fail."* The future of solar cells is as bright as the Sun. Photovoltaics is set to become a dominant complementary energy technology of the world's energy portfolio.

Acknowledgments I gratefully acknowledge my PhD advisors Dr. G. C. Jain and Dr. B. K. Das; my NPL colleagues at that time when I worked on polysilicon solar cells, Dr. S. N. Singh, Dr. D. K. Sadana, Dr. R. Kishor, Dr. R. Kotnala, Dr. N. Goel, and Mrs. Balakrishnan, for their valuable insights and support. In my subsequent PV research, I acknowledge the collaborations from Dr. Michael Jackson, RIT; Todd Barnum, Linton Technology; Dr. Ajeet Rohatgi, Georgia Institute of Technology, Founder and CTO, Suniva, Inc.; Dr. David Young, NREL; Dr. Rajendra Singh, Clemson University; and Dr. Nish Sonwalkar, Founder, SunDensity. I highly value the contributions of our students, Felipe Freire, Sidhant Grover, Alex Marshall, Karine Florent, Ronak Kamat, and Archana Devasia in the PV research work conducted in my group. I overwhelmingly thank my collaborators for their wealth of knowledge and support. This work could not have been done without the funding support from agencies—National Science Foundation (via the Silicon Solar Consortium), Department of Energy, and from the industry. I express my sincere gratitude to my family for their steadfast support all along my career.

References

1. National Renewable Energy Laboratory, "Best research-cell efficiency chart," 2021 [Online]. Available: https://www.nrel.gov/pv/cell-efficiency.html
2. D. M. Chapin, C. S. Fuller, and G. L. Pearson, "A new silicon p-n junction photocell for converting solar radiation into electrical power," *J. Appl. Phys.*, vol. 25, no. 5, p. 676, 1954.
3. M. Wolf, "Historical development of solar cells," in *Proceedings of the 25th Power Sources Symp.*, pp. 120–124, May 1972.
4. R. L. Easton and M. J. Votaw, "Vanguard I IGY satellite (1958 beta)", *Rev. Sci. Instrum.*, vol. 30, pp. 70–75, Feb. 1959.
5. M. Green, "Silicon photovoltaic modules: A brief history of the first 50 years," *Prog. Photovolt: Res. Appl.*, vol. 13, no. 5, pp. 447–455, 2005.
6. H. J. Queisser, "Slow solar ascent," in *Advances in Solid State Physics*, 1st ed, vol. 44, Berlin, Germany: Springer, pp. 3–12, 2004.
7. M. Green, "Forty years of photovoltaic research at UNSW," in *Journal and Proceedings of the Royal Society of New South Wales*, vol. 148, no. 455/456, pp. 2–14, 2015.
8. Solar Energy Technologies Office, "The sunshot initiative." Energy.gov. https://www.energy.gov/eere/solar/sunshot-initiative (accessed Apr. 20, 2021).
9. G. C. Jain, B. K. Das, and S. Kumari, "On the origin of core losses in an Mn-Zn ferrite with appreciable silica content," *J. Appl. Phys.*, vol. 49, no. 5, p. 2894–2897, May 1978.

10. S. N. Singh, S. Kumari, and G. C. Jain, "Development of low cost polycrystalline silicon solar cells for terrestrial applications," in *Photovolt. Solar Energy Conference*, Cannes, France, pp. 615–619, Oct. 1980.
11. W. Shockley and H. J. Queisser, "Detailed balance limit of efficiency of *p-n* junction solar cells," *J. Appl. Phys*., vol. 32, no. 3, pp. 510–519, 1961.
12. https://www.lmpv.nl/db/
13. A. Polman, M. Knight, E. G. Garnett, B. Ehrler, and W. C. Sinke, "Photovoltaic materials: Present efficiencies and future challenges," *Science,* vol. 352, no. 6283, p. 307–317, 2016. DOI: https://doi.org/10.1126/science.aad4424.
14. J. Liu, Y. Yao, S. Xiao, and X. Gu, "Review of status developments of high-efficiency crystalline silicon solar cells," *J. Phys. D: Appl. Phys.*, vol. 51, no. 12, 2018, Art. no. 123001.
15. X. Sun, M. R. Khan, C. Deline, and M. A. Alam," Optimization and performance of bifacial solar modules: A global perspective", *Applied Energy*, vol. 212, pp. 1601–1610, Feb. 2018
16. B. Kloter, D. Buß, A. Hussack, P. Kowalzik, S. Peters, M. Schutze, E. Stegemann, J. Muller, "Current status of high-efficiency Q.ANTUM technology at Hanwha Q CELLS", *2013 IEEE 39th Photovoltaic Specialists Conference (PVSC)*, 2013, pp. 1246–1248, doi: https://doi.org/10.1109/PVSC.2013.6744366.
17. M. Woodhouse, B. Smith, A. Ramdas, and R. Margolis., "Crystalline silicon photovoltaic module manufacturing costs and sustainable pricing: 1H 2018 benchmark and cost reduction roadmap," National Renewable Energy Laboratory, Golden, CO, USA, 2019. [Online]. Available: https://www.nrel.gov/docs/fy19osti/72134.pdf
18. Independent Commodity Intelligence Services, "Polysilicon (solar grade) methodology – September 2013," icis.com. [Online]. Available: https://www.icis.com/compliance/documents/polysilicon-solar-grade-methodology-september-2013/
19. G. Fisher, M. R. Seacrist, and R. W. Standley, "Silicon crystal growth and wafer technologies," *Proceedings of the IEEE*, vol. 100, Special Centennial Issue, pp. 1454–1474, May 2012, doi: https://doi.org/10.1109/JPROC.2012.2189786.
20. S. Schwinde, M. Berg, and M. Kunert, "New potential for reduction of kerf loss and wire consumption in multi-wire sawing," *Solar Energy Materials and Solar Cells*, vol. 136, pp. 44–47, May 2015.
21. TaiyangNews Webinar, "500W+ Solar Modules 2020", taiyangnews.info. http://taiyangnews.info/reports/500w-solar-modules-2020/ (accessed Apr. 25, 2021).
22. Vincent Shaw, "Big news as Zhonghuan Semiconductor unveils 12-inch super wafer", PV Magazine, Aug. 16, 2019. [online]. Available: https://www.pv-magazine.com/2019/08/16/big-news-as-zhonghuan-semiconductor-unveils-12-inch-super-wafer/ (accessed Jul 17, 2021).
23. Linton Crystal Technologies, https://www.lintoncrystal.com/ (accessed Jul 17, 2021).
24. J. Schmidt and K. Bothe, "Structure and transformation of the metastable boron- and oxygen-related defect center in crystalline silicon," *Physical Rev. B*, vol. 69, no. 2, Jan. 2004, Art. no. 024107.
25. N. E. Grant *et al*., "Gallium-doped silicon for high-efficiency commercial passivated emitter and rear solar cells," *Sol. RRL*, vol. 5, Art. no. 2000754, 2021.
26. S. K Kurinec, C. Bopp, and H. Xu, "Emergence of continuous Czochralski (CCZ) growth for monocrystalline silicon photovoltaics," in *Emerging Photovoltaic Materials: Silicon & Beyond*, S. K Kurinec, Ed., New York, NY: Wiley, 2018, ch. 1, sec. 1, pp. 4–19.
27. "Module Materials," PVEducation.com. [Online] Available: https://www.pveducation.org/pvcdrom/modules-and-arrays/module-materials
28. H. Hanifi, J. Schneider, and J. Bagdahn, "Reduced shading effect of half-cell modules –Measurements and simulations" in *31st Eur. Photovoltaic Solar Energy Conference and Exhibition*, Sep. 2015. [Online]. Available: https://www.researchgate.net/publication/283488492
29. S. Braun, G. Hahn, R. Nissler, C. Pönisch, and D. Habermann, "The multi-busbar design: An overview" *Energy Procedia*, vol. 43, pp. 86–92, 2013, doi: https://doi.org/10.1016/j.egypro.2013.11.092.

30. B. L. Allsopp *et al.*, "Towards improved cover glasses for photovoltaic devices," *Prog. Photovolt. Res. Appl.*, vol. 28, no. 11, pp. 1187–1206, 2020.
31. L. Rodríguez, "Bifacial modules: the future of solar PV? A comprehensive guide on financial and technical performance of the next hot thing in solar: RatedPower, Feb 21, https://ratedpower.com/blog/bifacial-modules/# (accessed Jul. 17, 2021).
32. R. Rapier, "Transmitting solar power underneath an ocean," *Advanced Energy*, Nov. 2020. [Online]. Available: https://4thgeneration.energy/transmitting-solar-power-underneath-an-ocean/
33. U.S. Dept. of State, "Strategic Defense Initiative (SDI)," 1983. [Online]. Available: https://2001-2009.state.gov/r/pa/ho/time/rd/104253.htm
34. A. Devasia and S. Kurinec, "Teaching solar cell I-V characteristics through SPICE modeling," *Am. J. Phys.*, vol 79, no. 12, pp. 1232–1239, Dec. 2011, doi: https://doi.org/10.1119/1.3636525.
35. R. A. Kamat, "Engineered emitters for improved silicon photovoltaics," M.S. Thesis, Dept. Elect. Eng., Rochester Inst. Tech., Rochester, NY, USA, 2016. [Online]. Available: https://scholarworks.rit.edu/theses/9337
36. A. Kale E. Beese, T. Saenz, E. Warren, W. Nemeth, D. Young, A. Marshall, K. Florent, S. Kurinec, S. Agarwal, and P. Stradins, "Study of nickel silicide as a copper diffusion barrier in monocrystalline silicon solar cells," in *2016 IEEE 43rd Photovoltaic Specialists Conference (PVSC)*, pp. 2913–2916, 2016, doi: https://doi.org/10.1109/PVSC.2016.7750190.
37. A. Marshall, K. Florent, A. Tapriya, B. G. Lee, S. K. Kurinec, and D. L. Young, "Nickel silicide metallization for passivated tunneling contacts for silicon solar cells," in *2016 IEEE 43rd Photovoltaic Specialists Conference (PVSC)*, pp. 2479–2482, 2016, doi: https://doi.org/10.1109/PVSC.2016.7750089.
38. S. Grover, S. Sahu, P. Zhang, K. O. Davis, and S. K. Kurinec, "Standardization of specific contact resistivity measurements using transmission line model (TLM)," in *2020 IEEE 33rd International Conference on Microelectronic Test Structures (ICMTS)*, Edinburgh, Scotland, UK, 2020, pp. 1–6, Apr. 2020. doi: https://doi.org/10.1109/ICMTS48187.2020.9107911.
39. F. Freire, R. Dias, T. Trabold, and S. K. Kurinec, "Performance analysis of a "green" building photovoltaic system," in *2016 IEEE 43rd Photovoltaic Specialists Conference (PVSC)*, 2016, pp. 2657–2660, doi: https://doi.org/10.1109/PVSC.2016.7750131.
40. S. K. Kurinec, M. Kucer, and B. Schlein, "Monitoring a photovoltaic system during the partial solar eclipse of August 2017" *Eur. J. Photovolt.*, vol. 9, 2018, Art. no. 7.
41. F. Freire, S. Melcher, C. G. Hochgraf, and S. K. Kurinec, "Degradation analysis of an operating PV module on a farm sanctuary," *J. Renew. Sust. Energy,* vol. 10, no. 1, 2018, Art. no. 013505, doi: https://doi.org/10.1063/1.4994565.
42. SunDensity, https://www.sundensity.net/
43. Fraunhofer Institute for Solar Energy Systems, "Photovoltaics Report," ISE, Feb. 2020. [Online]. Available: www.ise.fraunhofer.de/content/dam/ise/de/documents/publications/studies/Photovoltaics-Report.pdf
44. Z. Zhou and M. Carbajales-Dale, "Assessing the photovoltaic technology landscape: efficiency and Energy Return on Investment (EROI)," *Energy Environ. Sci.*, vol. 11, no. 3, pp. 603–608, 2018.
45. F. Liu and J.C.J.M. van den Bergh, "Differences in CO2 Emissions of Solar PV Production among Technologies and Regions: Application to China, EU and USA," *Energy Policy*, vol. 138, 2020, Art. no. 111234.
46. A. Jäger-Waldau, "Snapshot of photovoltaics—February 2020," *Energies*, vol. 13, no. 4, pp. 930–937, 2020.
47. N. Haegel, H. A. Atwater, T. Barnes, and C. Breyer, "Terawatt-scale photovoltaics: Transform global energy," *Science*, vol. 364, no. 6443, pp. 836–838, May 2019, doi: https://doi.org/10.1126/science.aaw1845.
48. IEA, "Solar PV," IEA.com, Paris, 2020. [Online]. Available: https://www.iea.org/reports/solar-pv
49. https://www.anu.edu.au/news/all-news/anu-scientists-set-new-record-with-bifacial-solar-cells

50. S. Maldonado, “The Importance of new “sand-to-silicon” processes for the rapid future increase of photovoltaics”, *ACS Energy Letters* 2020 *5* (11), 3628–3632, DOI: https://doi.org/10.1021/acsenergylett.0c02100
51. D. Brooks, “A solar panel in the New Hampshire woods is old enough to run for president”, Concordmonitor.com, Jun. 26, 2018. [Online]. Available: https://www.concordmonitor.com/oldest-solar-panel-NH-power-18318376

Santosh K. Kurinec is a Professor in the Department of Electrical and Microelectronic Engineering at Rochester Institute of Technology (RIT). She is a Fellow of IEEE and a member of the New York Academy of Sciences. She received her Ph.D. in Physics from University of Delhi, India, and worked as a Scientist at National Physical Laboratory, New Delhi. She joined the Department of Materials Science and Engineering at the University of Florida as a Postdoctoral Research Associate. Prior to joining RIT, she was Assistant Professor of Electrical Engineering at Florida State University/Florida A & M University College of Engineering in Tallahassee, FL. Her current research activities include advanced integrated circuit materials and photovoltaics. She received the 2012 IEEE Technical Field Award for integrating research in teaching to prepare microelectronic engineers for future challenges. She was inducted in the Women in Technology International Hall of Fame in 2018. She has over 120 publications in research journals and conference proceedings. Her recently edited books are *Energy Efficient Computing & Electronics: Devices to Systems*, and *Nanoscale Semiconductor Memories: Technology and Applications*, and *Emerging Photovoltaic Materials: Silicon & Beyond*.